# Helicopter handling qualities analysis using a synthetic eddy turbulence model

Sergio Henriquez Huecas
S.Henriquez-Huecas@liverpool.ac.uk
University of Liverpool

Prof. Mark White
mdw@liverpool.ac.uk
University of Liverpool

Prof. George Barakos
George.Barakos@glasgow.ac.uk
University of Glasgow

A turbulence model for flight simulation applications based on the synthetic eddy method (SEM) is introduced and evaluated through a study of impact of turbulence on aircraft handling and results from the trials will be presented. The turbulence model is derived from a Synthetic Eddy Model (SEM) first proposed by Jarrin et al. [1] to generate realistic velocity fluctuations at the inflow of CFD simulations. A short summary of the model and its implementation follows. A more detailed description is provided in Ref. [2].
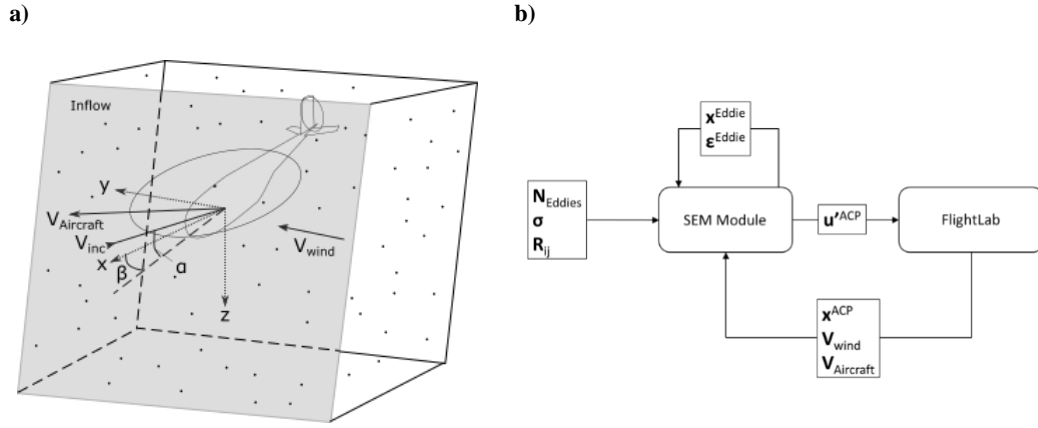
Figure 1: a) Diagram of the control volume used for the synthetic eddy method. b) Flow chart of data exchanged between the SEM module and FLIGHTLAB.

A box–shaped control volume is defined around the aircraft and filled by a random uniform distribution of turbulent eddies which generate flow disturbances at the aircraft's model aerodynamic computation points (ACPs) (see Figure 1). The distribution of eddies is defined by their strength, defined by the Reynolds stress tensor, $Re_{ij} = \langle u'_i u'_j \rangle$, their decay strength or size, $\boldsymbol{\sigma} = [\sigma_x, \sigma_y, \sigma_z]$, i.e. the distance within which the eddy generates velocity disturbances and the shape function $f_{\sigma(x)}(x - x^k)$, which relates the shape and size of the eddies, σ_i, with the decay of their effect with distance. The total number of eddies is set as $N_{Eddies} = \frac{V_B}{\sigma_x * \sigma_y * \sigma_z}$, in this manner the control volume is completely filled with eddies.

At each time step an eddy located on x^k generates a turbulent velocity perturbation on an ACP located at x^{ACP}. The total induced turbulence on each ACP is obtained by adding the contribution of each eddy:

$$u'^{ACP}_i = \frac{1}{\sqrt{N}} \sum_{k=1}^{N_{Eddies}} A_{ij} \varepsilon^k_j f_\sigma(x^{ACP} - x^k) \qquad \mathbf{1}$$

Where ε^k_j is a randomly assigned sign and $\boldsymbol{A}$ is the Cholesky decomposition of the Reynolds stress tensor. Adjustment of the Reynolds Stress tensor controls the resulting turbulence intensity (see Figure 2 a)), while the shape function $f_{\sigma(x)}(x - x^k)$ and the shape and size of the eddies, σ_i,

defines the resulting turbulence spectra (see Figure 2 b)). Values for these parameters can be obtained from measurements or CFD simulations [3], [4].

a)

b)
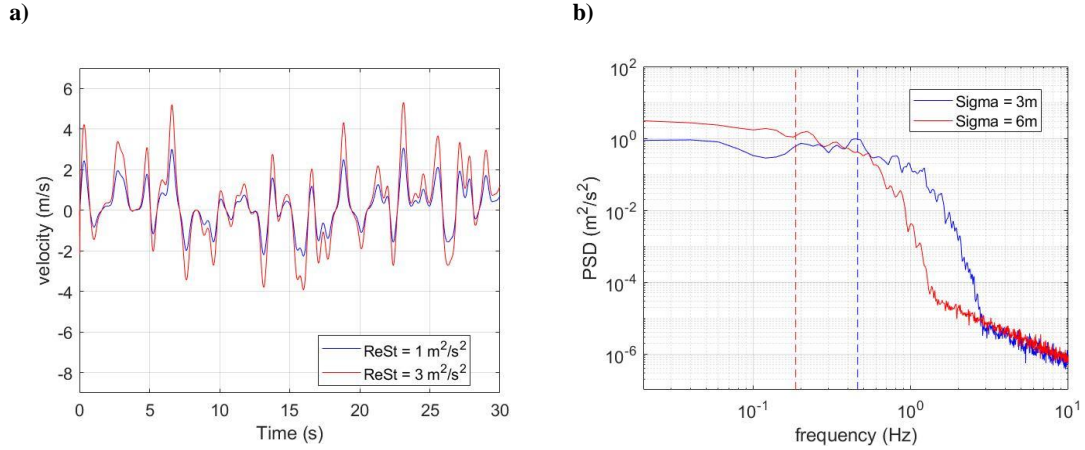
Figure 2: Effect of SEM parameters on generated turbulence: a) changes in value of Reynolds Stresses, b) changes in eddy size. Vertical dashed lines indicate average frequencies.

The physical location of the eddies surrounding the aircraft is preserved and updated on each time step. Displacing them using information on the environmental flow and the new location of the aircraft. Eddies falling outside the control volume at the start of the time step are regenerated at a random location at the inflow. This results in the automatic correlation of turbulent flow velocities across the aircraft.

An adaptation of the SEM to work with multiple series of eddies of different strength and size has been implemented. The algorithm used is an adaptation to the one described by Y. Luo [4]. The size and strength of the eddies in each series are given by:

$$\boldsymbol{\sigma^m} = q_m * \sigma$$

$$\boldsymbol{A^m} = \sqrt{\boldsymbol{p_m}} * \boldsymbol{A}$$

2

where q_m and p_m are scaling values relating eddy size and Reynolds Stress tensor to a reference value. The control volume is therefore populated by a uniform distribution of $N^m = \frac{V_B}{\sigma_x^m * \sigma_y^m * \sigma_z^m}$ eddies of each series. In average each ACP will be in range of about eight eddies. For very large eddies, less than this amount might fit within the control volume. So an additional control volume, large enough to satisfy this requirement is defined for this series.

Each individual series presents the characteristic behaviour and average frequency for its eddy strength and size and the resulting induced turbulence is the sum of the turbulence generated by each of the eddy series:

$$u'^{ACP}_i = \sum_{m=1}^{N_{Series}} \left(\frac{1}{\sqrt{N^m}} \sum_{k=1}^{N^m_{Eddies}} A^m_{ij} \varepsilon^k_j f_{\sigma_m}(\boldsymbol{x}^{ACP} - \boldsymbol{x}^k) \right)$$

3

By adequately relating eddy strength and size for each series, it is possible to adjust the slope of the resulting turbulence power density with frequency.

The number of required operations on each timestep scales proportional to the number of eddies in the model; this becomes the most relevant parameter for computational performance. Through adjustment of the aircraft model time step, real-time capability of the model in its current implementation has been achieved for up to 400 eddies. Initial testing of the synthetic eddy turbulence showed the feasibility of using the model for piloted flight simulation [2] and the resulting disturbances had a measurable impact on aircraft handling and pilot workload.

A flight simulation testing campaign is currently ongoing at the University of Liverpool's flight simulator [5], using a FLIGHTLAB [6] model of a Bell412 [7] helicopter in order to confirm those findings. Two main tasks are being tested. A precision hover mission task element (MTE) as

defined in ADS – 33 [8] and a custom designed steady and level forward flight task. The runs have been performed under different turbulence conditions obtained by changing size, strength of the eddies as well as testing the impact of the multi-scale eddy induced turbulence.

Analysis of the hover task reveals significant impact of the turbulence on the achieved performance in hover. Increasing values of Re_{ij}, which results in increased turbulence intensity, or larger eddy sizes, which produce turbulence of lower average frequency, led to higher pilot workload ratings on the Bedford workload scale [9]. Pilot feedback and analysis of test data pointed towards collective control during the station keeping segment of the MTE being the dominant focus of his effort and attention.

These findings are summarized in Figure 3 a) which shows increased RMS of pilot inputs in the collective against RMS of turbulence during the station keeping phase correlating with increasing pilot workload ratings. Figure 3 b) also shows this trend of increased workload for turbulence of increasing strength and lower frequency. The impact of including multiple series of eddies seems to induce more complex pilot behaviour, but a similar overall trend.

a)   b)
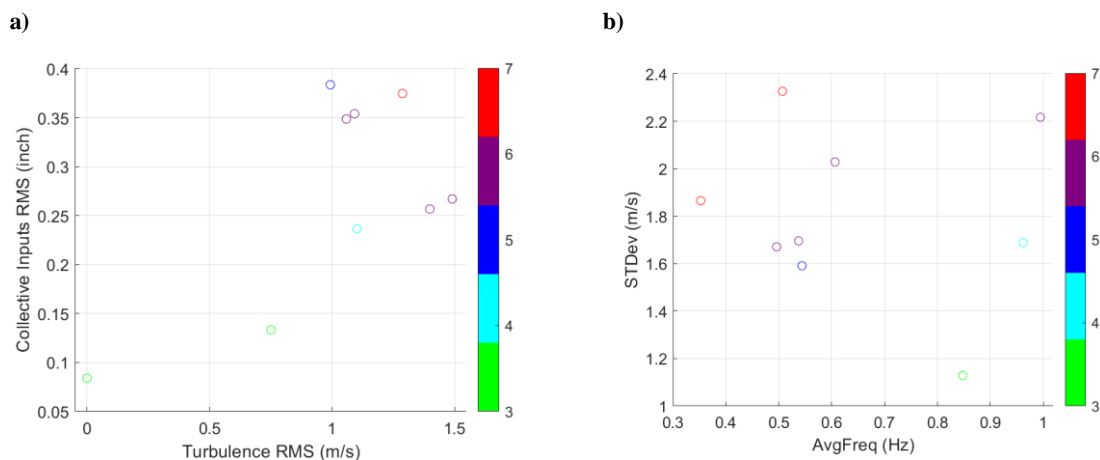

Figure 3: Impact of turbulence during the station keeping phase of the hover MTE. a) RMS of pilot collective inputs against RMS of turbulence velocities, marker color indicates assigned pilot workload ratings b) Assigned pilot workload ratings, given by marker color, against turbulence standard deviation and average frequency.

A second steady and level forward flight task was also tested. The pilot was tasked with maintaining flight speed at 40kts and 60 kts respectively and not to exceed a maximum altitude. Boundaries for lateral and altitude deviations were based on those defined for the ADS – 33 acceleration – deceleration MTE. While boundaries for deviations in flight speed where defined based on deviations observed in the initial feasibility trials [2].

Initial analysis of the results shows a much more limited impact of turbulence on workload and task performance during forward flight, especially at higher flight speed. Overall, the pilot was able to keep deviations within desired limits in all cases. Pilot feedback suggests that his effort and attention shifted from collective to roll and yaw, in part because requirements for altitude deviations in this task are much less stringent.

Increased turbulence intensity still results in increased workload ratings for all cases. Interestingly, the impact of eddy size seems to be most relevant at an intermediate size (σ = 6m) (see Figure 4). With the pilot awarding higher workload ratings of 5 and recording data showing larger lateral deviations under this condition (Figure 5). A similar effect was observed during the translation phase of the hover task, with the pilot reporting higher difficulty in maintaining a constant approach rate and altitude.

a)   b)
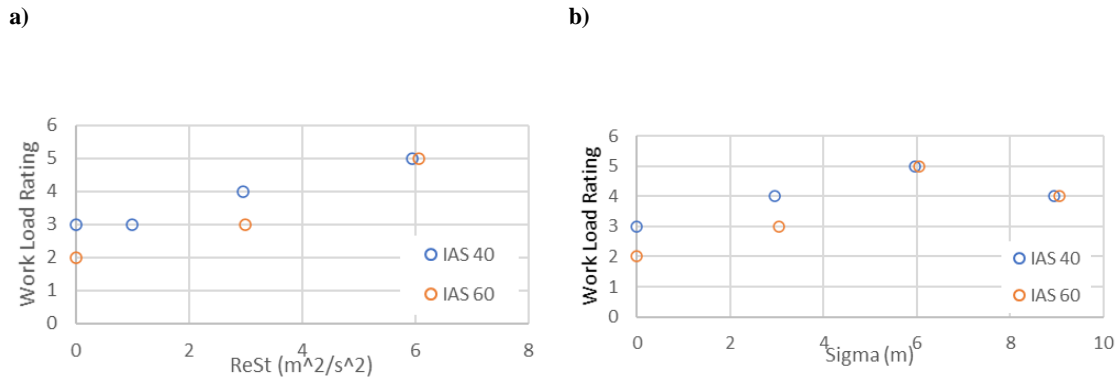
Figure 4: Assigned pilot workload ratings during the forward flight task at 40 and 60 kts against a) Values of Reynolds stress tensor. b) eddy size.
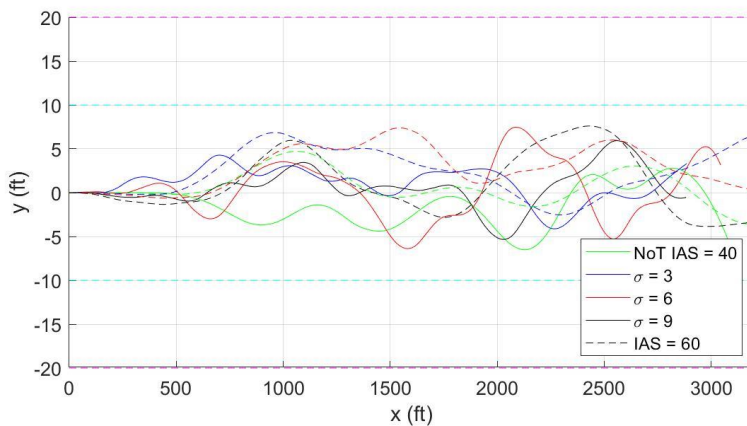
Figure 5: Lateral deviations during the forward flight tasks at 40kts and 60 kts under different eddie sizes. Horizontal dashed lines in cyan and magenta indicate desired and adequate limits.

Further analysis of these results is still ongoing to inform the best conditions for use of the SEM turbulence model and results will be presented in the forthcoming presentation.

References

[1]   N. Jarrin, S. Benhamadouche, D. Laurence, and R. Prosser, "A synthetic-eddy-method for generating inflow conditions for large-eddy simulations," *Int. J. Heat Fluid Flow*, vol. 27, no. 4, pp. 585–593, 2006, doi: 10.1016/j.ijheatfluidflow.2006.02.006.

[2]   S. Henriquez Huecas, M. White, and G. Barakos, "A turbulence model for flight simulation and handling qualities analysis based on a synthetic eddy method," *76th Vert. Flight Soc. Forum, Virginia Beach, VA*, 2020.

[3]   N. Jarrin, R. Prosser, J. C. Uribe, S. Benhamadouche, and D. Laurence, "Reconstruction of turbulent fluctuations for hybrid RANS/LES simulations using a Synthetic-Eddy Method," *Int. J. Heat Fluid Flow*, vol. 30, no. 3, pp. 435–442, 2009, doi: 10.1016/j.ijheatfluidflow.2009.02.016.

[4]   Y. Luo, H. Liu, Q. Huang, H. Xue, and K. Lin, "A multi-scale synthetic eddy method for generating inflow data for LES," *Comput. Fluids*, vol. 156, pp. 103–112, 2017, doi: 10.1016/j.compfluid.2017.06.017.

[5]   M. D. White, P. Perfect, G. D. Padfield, A. W. Gubbels, and A. C. Berryman, "Acceptance testing and commissioning of a flight simulator for rotorcraft simulation fidelity research," *Proc. Inst. Mech. Eng. Part G J. Aerosp. Eng.*, vol. 227, no. 4, pp. 663–686, 2013, doi: 10.1177/0954410012439816.

[6]   R. W. Du Val and C. He, "Validation of the FLIGHTLAB virtual engineering toolset," *Aeronaut. J.*, vol. 122, no. 1250, pp. 519–555, Apr. 2018, doi: 10.1017/aer.2018.12.

[7]   P. Perfect, M. D. White, G. D. Padfield, and A. W. Gubbels, "Rotorcraft simulation fidelity: new methods for quantification and assessment," *Aeronaut. J.*, vol. 117, no. 1189, pp. 235–282, Mar. 2013, doi: 10.1017/S0001924000007983.

[8]   "Aeronautical Design Standards - Performance Specification Handling Qualities Requirements for Military Rotorcraft," *United States Army Aviat. Missile Command*, vol. E-PRF, 2000.

[9]   A. H. Roscoe and A. H. Ellis, "Technical Report TR 90019: A subjective rating scale for assessing pilot workload in flight: A decade of practical use," *R. Aerosp. Establ.*, 1990.